

Vibrational absorption of tunneling molecular defects in crystals.*

II. Tunneling molecules under applied stress (KCl:CN⁻)

Fritz Lüty

Physics Department, University of Utah, Salt Lake City, Utah 84112

(Received 19 October 1973)

The general considerations about the vibrational absorption of tunneling molecules, developed in Paper I of this work, are applied and tested, using CN⁻ defects in KCl. In previous work on this system the vibrational absorption of CN⁻ was reported to be strongly broadened by an unresolved tunneling splitting, and to show pure zero-moment changes under applied stress. The tunneling model, however, predicts additionally characteristic anisotropic changes of the spectral shape under applied field or stress for any absorption, broadened by orientational tunneling. A thorough experimental reinvestigation of this system at low temperatures yields results which agree with the predictions from the tunneling model. For low CN⁻ concentration, the first- and second-harmonic vibrational absorption (at 5 and 2.5 μm) consists of a resolved double structure, caused by the reorientational tunneling of the molecule in the crystal (tunneling splitting $\Delta = 1.2 \text{ cm}^{-1}$). The application of uniaxial stress of different symmetry is found to produce two basic effects: Second-moment absorption changes (due to quantum-mechanical mixing of the tunneling states by the stress), and zero-moment changes (due to classical elastic dipole alignment). The observed pronounced anisotropy of these effects yield both independently a (cigar-shaped) $\langle 111 \rangle$ elastic dipole model. These results disagree with the (pancake-shaped) $\langle 100 \rangle$ elastic dipole, derived from the earlier elasto-optical work, which has been the basis of the so far generally accepted $\langle 100 \rangle$ defect model. Consequences of this symmetry change for the interpretation of several previous investigations on KCl:CN⁻ will be discussed.

I. INTRODUCTION

In Paper I of this work¹ we have discussed the question of electric-field-induced absorption changes for tunneling paraelectric defects, which have been found to be of two kinds: (a) Changes in the *absorption strength* for light of different polarization, due to field alignment of the dipoles and their permanent anisotropic absorption components. This well-known *classical* alignment dichroism thus produces *zero-moment changes* of the absorption. (b) Changes in the *spectral structure* of the absorption due to the transformation of the original tunneling states into localized dipole states with different selection rules. This *quantum-mechanical* effect produces *second-moment decreases* of the main vibrational absorption, which are highly anisotropic in terms of dipole, field, and polarization direction.

If tunneling is the underlying mechanism for reorientation, the existence of the effect b is the necessary *precondition* for the existence of the alignment effect a. Experimentally, however, the quantum-mechanical effect b will be detectable only if the tunneling splitting Δ gives a measurable contribution to the width H of the absorption in question, i.e., for system with sizable tunneling splitting and narrow absorptions.

One of the largest tunneling splittings for molecular defects has been found for CN⁻ in KCl. Several experiments with various techniques² gave

consistent evidence for a large tunneling splitting of $1.0\text{--}1.5 \text{ cm}^{-1}$. In general agreement with this, the vibrational absorption at 5 μm was found to show a low-temperature width of about 2.5 cm^{-1} , which was interpreted to arise from the large unresolved tunneling splitting.³ Under application of uniaxial stress³ and electric fields,^{4,5} absorption changes were observed, which were reported to consist of pure changes of the absorption strength (zero-moment changes).

It is evident from our discussion in Paper I that these results are not in full agreement with the tunneling model (particularly for the electric field case,^{4,5} where all experiments have been done in the $pE < \Delta$ range). An absorption band with a width caused mostly by orientational tunneling, should display (besides the classical zero-moment changes) pronounced anisotropic changes of the absorption *shape* under applied E or S , due to the field- or stress-mixing of the initial tunneling states and the resulting changes in the optical transitions. The KCl:CN⁻ system with its large tunneling splitting should be an ideal test case for the optical detection of these quantum-mechanical effects.

A second motivation for the reinvestigation of the KCl:CN⁻ system is a lack of consistency between several previous experiments in terms of the derived *electric and elastic dipole symmetry*. (This is in marked contrast to the impressive agreement achieved with a large variety of experi-

mental techniques for other paraelectric and para-elastic defect systems, like Li^+ in KCl .²) The previously reported elasto-optical effect³ in $\text{KCl}:\text{CN}^-$ was found highest for $\langle 100 \rangle$ stress, which was taken as an indication for $\langle 100 \rangle$ oriented dipoles (though an effect of more than $\frac{1}{3}$ relative size was found for $S_{(111)}$ as well). Ultrasonic measurements⁶ clearly showed a predominant coupling of the CN^- to T_{2g} phonons, thus definitely excluding a simple $\langle 100 \rangle$ elastic-dipole model. The reported electro-optical effect,^{4,5} on the other hand, was found to have a sign opposite to the expected, consisting of zero-moment changes which would correspond to dipole alignment perpendicular to the field. Complicated, and for physical reasons unsatisfactory models ("modified Devonshire model"^{4,5} and the "Byer-Sack-model" with electric and elastic dipole axes lying perpendicular⁷) had to be used to integrate these results into a single defect model. In all papers since 1966 and in a recent comprehensive review article,² the elasto-optical experiment³ has been selected as *the* decisive one for the defect symmetry, so that a $\langle 100 \rangle$ defect model has been generally adopted for the interpretation of experimental results on this system.

The motivation for this work is therefore two-fold: (i) to test the predictions from the tunneling model on the stress-induced change of the absorption shape; (ii) to reinvestigate the elastic dipole alignment by measurements of the stress-induced integrated absorption.

Both measurements should yield independently, by their characteristic anisotropy, the CN^- defect symmetry, and thus clarify this unsettled question. The new results and conclusions, obtained in this work, clearly justify this reinvestigation.

II. EXPERIMENTAL TECHNIQUES

Three types of crystals were used for the investigation, grown under pure argon atmosphere from reagent grade or ultrapure KCl material. The crystals of type *A* were doped with 2×10^{-2} , crystals of type *B* with 6×10^{-2} and crystals of type *C* with 2×10^{-1} -Mol% KCN in the melt. From the measured CN^- vibrational spectra at liquid-nitrogen temperature (LNT) an actual content of 1×10^{-2} , 4.5×10^{-2} , and 1.5×10^{-1} -Mol% KCN for *A*, *B*, and *C*, respectively, were determined in the crystals. The oriented samples were cut and polished by the usual techniques with an orientational accuracy of about 2° . A stress optical He cryostat (like the one used in Ref. 8) with immersion of the crystal in He exchange gas was used for the investigation. All measurements of the fundamental vibrational absorption were performed

with a Beckman ir 12 instrument, using a gold wire polarizer in the sample beam. As the light of the instrument around 2000 cm^{-1} is strongly polarized, considerably more light intensity was available for horizontal polarization. Therefore the measurements with light polarized perpendicular (\perp) to the stress could be performed with higher resolution ($0.4\text{--}0.5 \text{ cm}^{-1}$) than the measurements with light polarized parallel (\parallel) to the stress ($0.9\text{--}1.5 \text{ cm}^{-1}$). The high-resolution (i.e., low-light-intensity) operation of the instrument allows reliable measurements of absorption or absorption changes *only* for small optical densities. Any measurements for $OD > 1$ have to be discarded as unreliable. The second-harmonic absorption was measured in the same cryostat using a Carey 14 instrument with the expanded ($OD\ 0\text{--}0.1$) scale. An additional interference filter with maximum transmission at $2.5 \mu\text{m}$ prevented the heating of the sample by the strong light of the ir2 range. Similar to the Beckman Instrument, the Carey is strongly \perp polarized. Therefore stress-optical measurements on the second-harmonic absorption could be performed with reasonable resolution only for \perp polarization.

III. EXPERIMENTAL RESULTS

The first measurements were attempted with samples from crystal type *C*, with the idea of reproducing roughly the CN^- concentration used in the prior elasto-optical work.³ For 2–4-mm optical thickness of the samples (necessary to achieve high-stress application) the peak of the low-temperature CN^- absorption was found to be far off scale (i.e., $OD \gg 1$).

Consequently, crystals of type *A* with one order of magnitude lower CN^- concentration were used for all stress-optical measurements on the fundamental vibrational absorption. Figure 1 shows the original graph of the first low-temperature measurement on this sample. In striking contrast to the earlier work, a splitting of the vibrational band into two components can be clearly detected below 16°K . At 4.5°K the two components are nearly fully resolved. The low energy component loses somewhat in strength compared to the high-energy component to lowest temperatures. The splitting between the two components was found to be $\delta = 2.4 \pm 0.1 \text{ cm}^{-1}$. The splitting was reproduced in more than a dozen low-temperature measurements on differently oriented samples of crystal type *A*, grown both from reagent-grade and ultrapure material.

The spectral structure of the vibrational absorption was then systematically studied for the three different CN^- concentrations, both in the fundamental and second harmonic absorption, using

samples of appropriate thickness. Figure 2 summarizes the results of an extended set of measurements: For the smallest CN^- concentration, which shows full resolution of the double structure in the fundamental absorption, a somewhat less resolved double structure (with the same energy separation) can be observed in the second-harmonic absorption. For the medium CN^- concentration, the double structure is still detectable (again better for the first harmonic absorption), but more washed out. For the highest CN^- absorption, both the first- and second-harmonic absorptions consist of a single broad band, with only a slight remaining indication of the original double structure. It is evident from this that interaction effects among CN^- dipoles are highly effective in washing out the double structure observed for low CN^- concentrations.

Figures 3–5 show measurements on the fundamental vibrational absorption for the low CN^- concentration under application of uniaxial stress in $\langle 100 \rangle$, $\langle 111 \rangle$, and $\langle 110 \rangle$ directions. It should be recognized that these are transposed smoothed-out curves from measurements with the smallest possible slit width, i.e., with a quite low signal-to-noise ratio (about 10:1 for \parallel , and 5:1 for \perp polarization). Therefore, neglecting finer details,

the following gross features can be recognized with reasonable certainty:

(a) Under $S_{\langle 100 \rangle}$ and \perp polarization (Fig. 3), the initial double structure is basically preserved though the separation between the two components becomes somewhat reduced.

(b) Under $S_{\langle 111 \rangle}$ and \perp polarization (Fig. 4), the double structure narrows quickly and changes into a single band, remaining however fairly broad in the absorption wings. An increase of the area can be recognized. At higher temperatures [Fig. 4(b)], where the double structure is washed out, $S_{\langle 111 \rangle}$ application produces a similar narrowing effect on the absorption.

(c) Under $S_{\langle 110 \rangle}$ (Fig. 5), two completely different behaviors are observed in the two inequivalent polarization directions \perp to $S[110]$. For $[1\bar{1}0]$ polarization [Fig. 5(a)] the double structure is transformed into a single line absorption which becomes extremely narrow for higher stress, far beyond the resolution limit of the instrument. This latter fact introduces severe errors in the measured *area* of the band (making it appear to decrease),⁹ which precludes any estimate about the stress-induced area change. For $[001]$ [Fig. 5(b)], the situation is completely different: the double structure remains preserved, even becoming

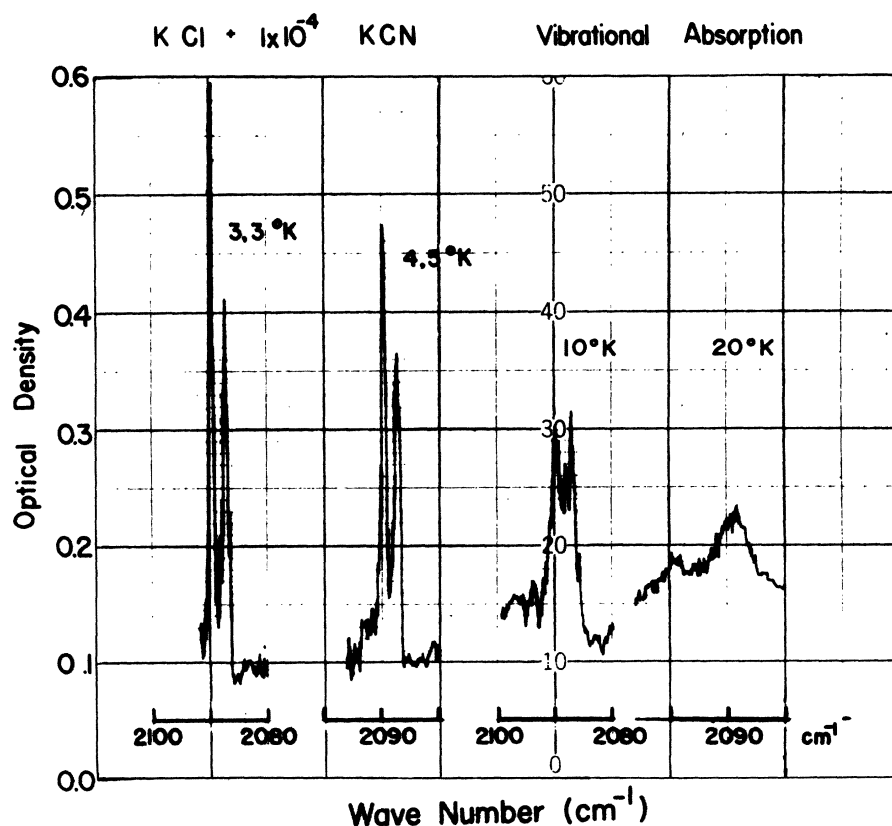


FIG. 1. Original graph of the absorption measurement on $\text{KCl} + 1 \times 10^{-4} \text{CN}^-$, at four different temperatures. (The relative CN^- concentration in this and all following figures is given in Mol parts KCN in the KCl crystal.)

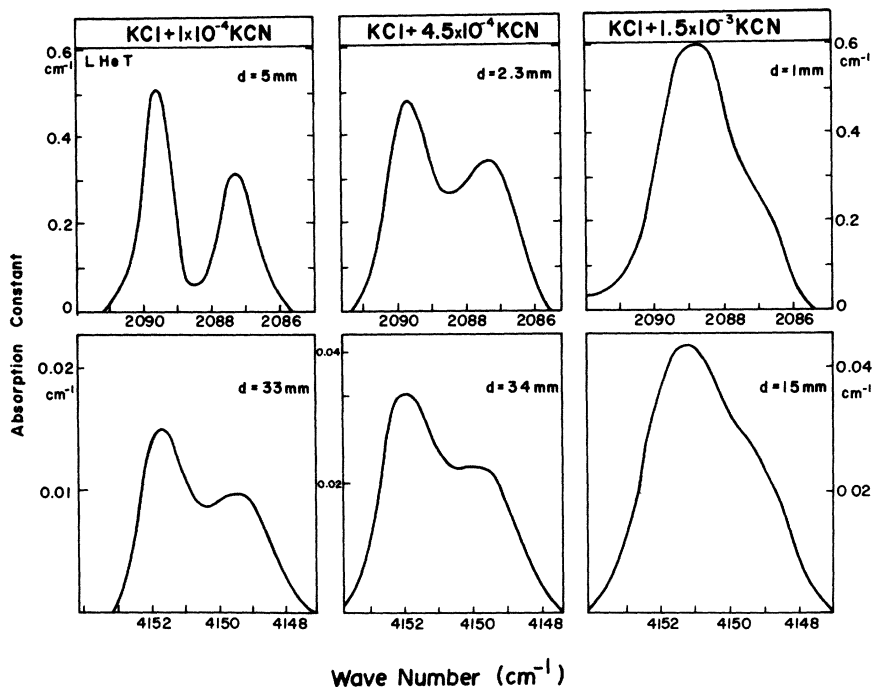


FIG. 2. Summary of low-temperature absorption measurements of the fundamental (upper part) and second-harmonic (lower part) vibrational absorption of CN^- in KCl, for crystals with three different CN^- concentrations, measured at 4.2 °K.

somewhat broader (and washed out) under stress.

Owing to the very small value of the second harmonic absorption (about a factor of 200 smaller than the fundamental), stress optical measurements on the second-harmonic absorption could be performed only using the crystal type C with the high CN^- concentration. For this case, the double structure is washed out by interaction effects (see Fig. 2) and only a single broad band is observed (Fig. 6). Stress application at low temperatures again produces pronounced and very anisotropic spectral changes in this absorption (all measured in \perp polarization). Application of $S_{(100)}$ and $S_{(110)}$ (measured in $\perp_{(001)}$) produce—within experimental error—no measurable spectral

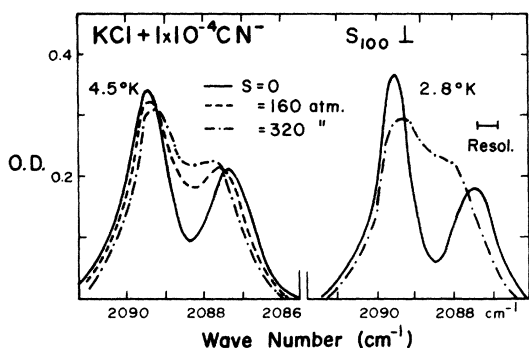


FIG. 3. Effect of $\langle 100 \rangle$ stress on the fundamental vibrational absorption spectrum of CN^- in KCl, measured for \perp polarization at two temperatures.

change in the broad absorption bands. $S_{(111)}$ and $S_{(110)}$ (measured in $\perp_{(1\bar{1}0)}$), however, cause a narrowing of the second harmonic band, with the effect being much more pronounced for $S_{(110)}$ in $\perp_{(1\bar{1}0)}$ polarization. Again it was observed qualitatively that these narrowing effects on the second harmonic absorption are present and can be measured at higher temperatures (~ 20 K) also.

In summary, Figs. 3–6 clearly show that stress application in different directions cause pronounced anisotropic changes of the spectral shape of both

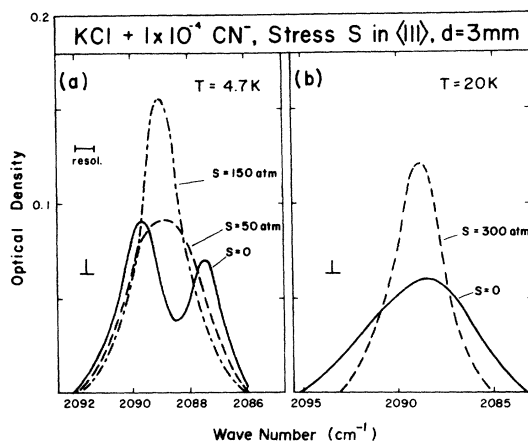


FIG. 4. Effect of $\langle 111 \rangle$ stress on the fundamental vibrational absorption spectrum of CN^- in KCl, measured for \perp polarization at two different temperatures.

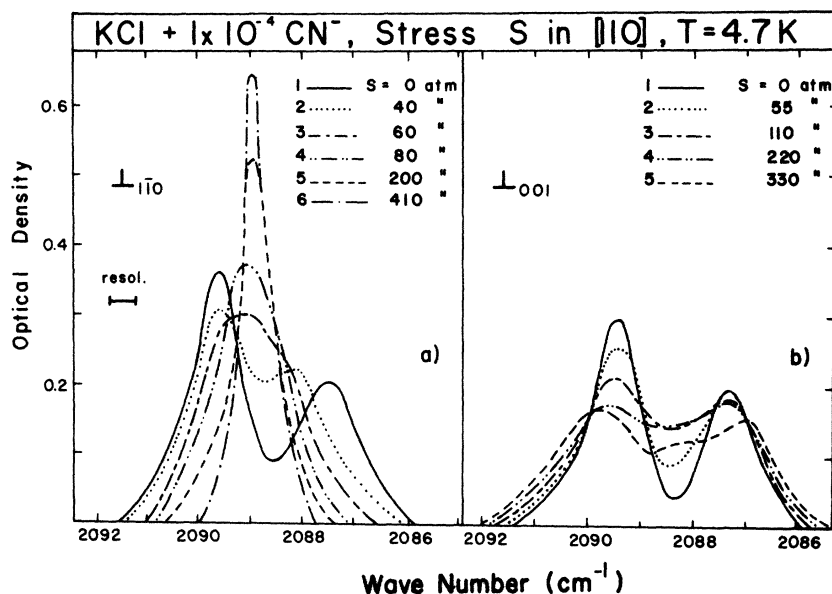


FIG. 5. Effect of $\langle 110 \rangle$ stress on the fundamental vibrational absorption spectrum of CN^- in KCl, measured at 4.7 °K for the two inequivalent polarization directions ($\perp_{\langle 1\bar{1}0 \rangle}$ and \perp_{001}), which lie perpendicular to the $\langle 110 \rangle$ stress axis.

the first and second harmonic absorption, both for crystals with low and high CN^- doping (i.e., with resolved and unresolved double structure).

A separate set of measurements was conducted with the aim to determine as accurately as possible merely the *change in the absorption area (zero moment)* under stress, neglecting all details of the spectral structure. Measurements of this type can easily produce misleading results, as one works here with absorptions with strong spectral changes under stress and an optical instrument at the resolution limit. Under these conditions a determination of the absorption area is virtually impossible for the stress and polarization directions, in which a strong stress-narrowing of the

band occurs [like for $S_{\langle 111 \rangle \perp}$ and $S_{\langle 110 \rangle (\perp_{\langle 1\bar{1}0 \rangle})}$ in Figs. 4 and 5(a)]. If this stress-narrowing produces a bandwidth $H(S)$ which becomes increasingly smaller compared to the spectral slit width, an apparent and erroneous decrease of the absorption band will show up.⁹ (We believe that this stress-narrowing in connection with improper resolution conditions produced in the early elastooptical work³ the apparent absorption decreases in \perp polarization, which are incompatible with our results.)

For the stress and polarization directions, without stress narrowing, however, relative zero-moment absorption measurements can be done with reasonable accuracy. Figure 7 gives an example for the medium-doped crystal. To achieve a better

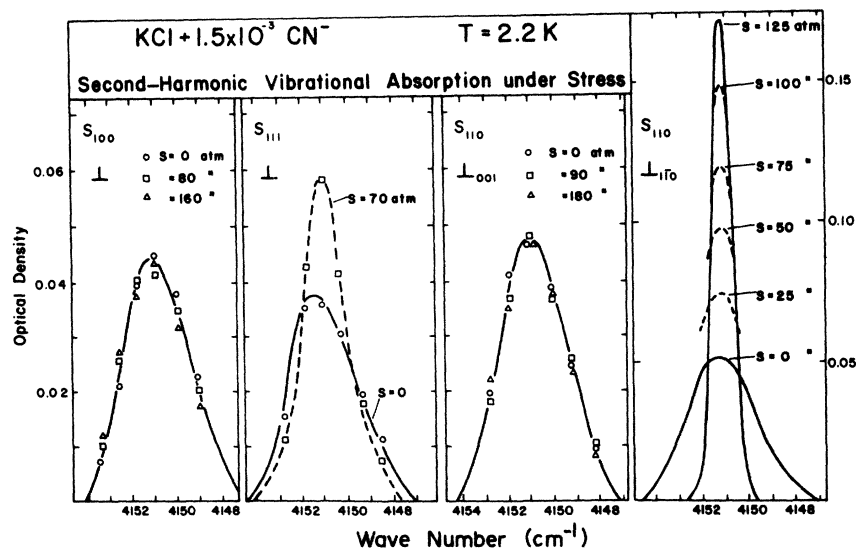


FIG. 6. Effect of uniaxial stress (applied in $\langle 100 \rangle$, $\langle 111 \rangle$, and $\langle 110 \rangle$ direction) on the second-harmonic absorption of CN^- in KCl, measured at 2.2 °K for \perp polarization.

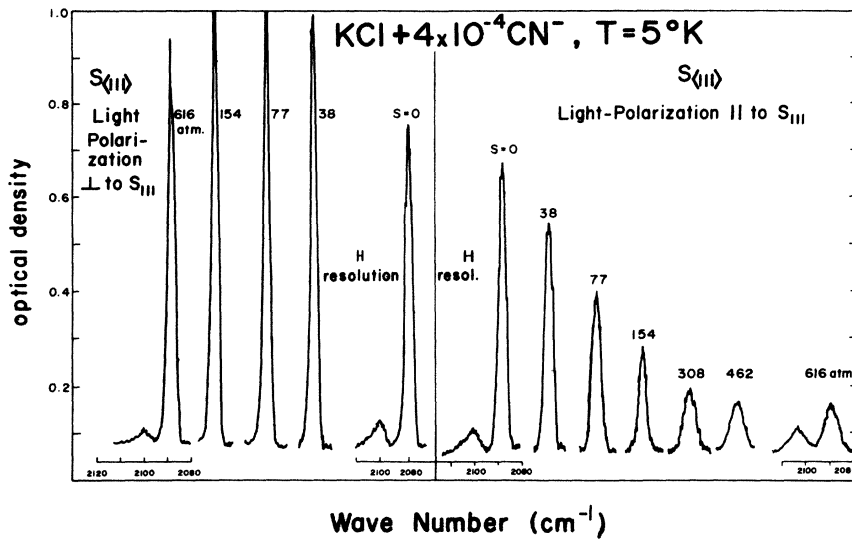


FIG. 7. Absorption spectra for $\text{KCl}:\text{CN}^-$ under various $S_{\langle 111 \rangle}$ values, measured in \parallel and \perp polarization at 5°K .

signal-to-noise ratio and easier integration, the slit was set to a somewhat larger value, so that the double structure was washed out and a single band appeared. Application of $S_{\langle 111 \rangle}$ produces the following effects: For \perp polarization the absorption narrows and increases (in agreement with Fig. 4), going quickly off scale. (Under large stress, i.e., very strong narrowing, it comes back into scale and seems to decrease, which is a clear example of an erroneous measurement under changing and improper resolution conditions!) For \parallel polarization the band decreases and broadens so that it can be measured (and integrated) with reasonable accuracy. Figure 8 shows also (for $S=0$ and $S=610$ atm) the small librational side band of the vibrational absorption at 2100 cm^{-1} . As can be seen qualitatively, this sideband increases for \parallel and

decreases for \perp polarization, opposite to the changes of the main absorption.

Similar experiments with $S_{\langle 100 \rangle}$ in \parallel and \perp polarization (not shown here) yielded, within the experimental accuracy, no change in the absorption area by the stress application. Figure 8 shows the results for $S_{\langle 110 \rangle}$ application, measured in \parallel and $\perp_{\langle 001 \rangle}$ polarization. While for $\perp_{\langle 001 \rangle}$ polarized light the absorption is very little affected by the stress, the absorption decreases to a very small residual value for the \parallel polarization.

The absorption area (or zero-moment $\langle K \rangle_S^0$) obtained by integration of these types of experimental curves, is plotted in summary in Fig. 9 for the different stress and polarization symmetries (normalized to the absorption area at zero stress $\langle K \rangle_{S=0}^0$).

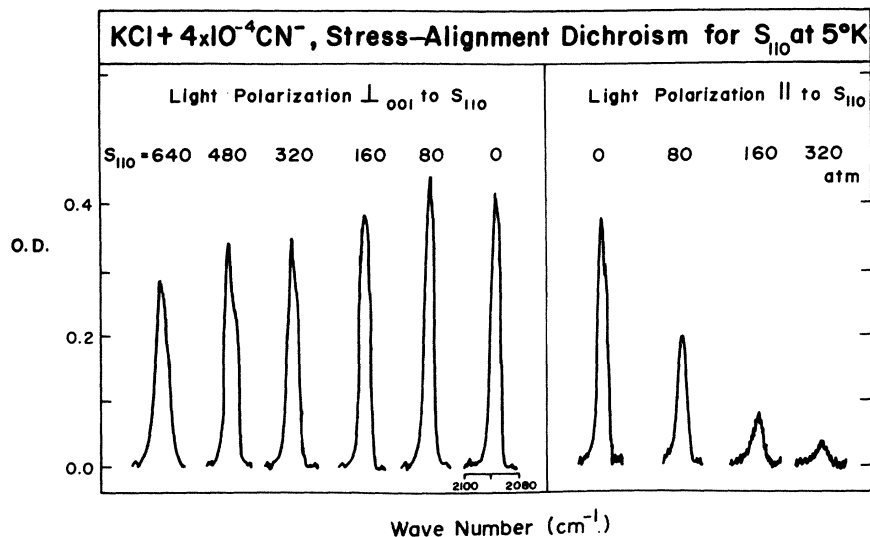


FIG. 8. Absorption spectra for $\text{KCl}:\text{CN}^-$ under various $S_{\langle 110 \rangle}$ values, measured in \parallel and $\perp_{\langle 001 \rangle}$ polarization at 5°K .

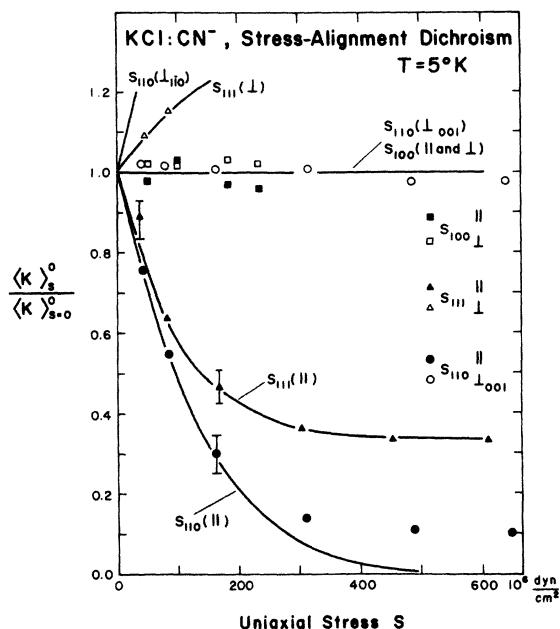


FIG. 9. Integrated CN^- absorption under stress $\langle K \rangle_S^0$ (normalized to the value at zero stress $\langle K \rangle_{S=0}^0$) as a function of the applied stress for different symmetries of stress and polarization. The curves have been calculated for a $\langle 111 \rangle$ elastic dipole model as described in the text.

IV. TUNNELING ELASTIC DIPOLE UNDER STRESS APPLICATION

Before we attempt an interpretation of the results from Sec. III, we need to develop the predictions from the tunneling model for the stress-induced spectral absorption changes of tunneling elastic dipoles (similar to what we have done for

the field-induced changes of tunneling electric dipoles in Paper I). Recognizing that experimentally we don't observe the weak "paraelastic sidebands" of the vibrational absorption under stress (Fig. 4 of Paper I), we limit all our considerations to the main vibrational transitions with a strength of the order one.

In Figs. 10-12 we illustrate for $\langle 100 \rangle$, $\langle 111 \rangle$, and $\langle 110 \rangle$ elastic dipoles the vibrational ground and excited states and their splitting by tunneling and by stress $S_{\langle 100 \rangle}$, $S_{\langle 111 \rangle}$, and $S_{\langle 110 \rangle}$. The allowed optical transitions (with strength of order 1) are indicated in the level diagram, and the resulting spectral absorption histograms for light polarized parallel (\parallel) and perpendicular (\perp) to the applied stress are given in the lower part of the figures. The transitions have been calculated from the dipole-matrix elements for optical transitions between the appropriate tunneling states under high-stress ($\alpha S > \Delta$) application. (All considerations are again limited, as in Paper I, to $kT \gg \alpha S$, i.e., the absence of stress alignment of the dipoles.)

The results, illustrated in Figs. 10-12 are qualitatively very similar to the ones obtained from the main vibrational transitions under field application in Paper I. Starting with the original absorption spectra from transitions between the pure tunneling states at $S = 0$ (which we have assumed to be optically resolved), we find that stress application will cause spectral changes in this absorption which are highly anisotropic in terms of the direction of the dipoles, the stress, and the polarization direction. Similar to the electric-field case, the stress-induced spectral changes of the main absorption consist of pure second-moment changes (decreases), i.e., a narrowing of the

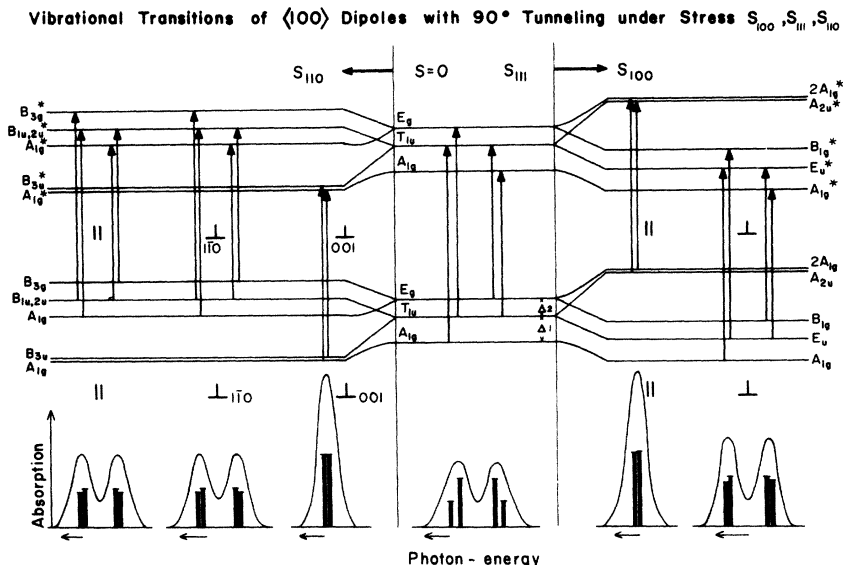


FIG. 10. Energy-level diagram and main optical transitions (with strength of order 1) for $\langle 100 \rangle$ dipoles with nearest-neighbor tunneling under applied stress $S_{\langle 100 \rangle}$, $S_{\langle 111 \rangle}$, and $S_{\langle 110 \rangle}$. The resulting spectral transition histograms for \parallel and \perp polarization are indicated.

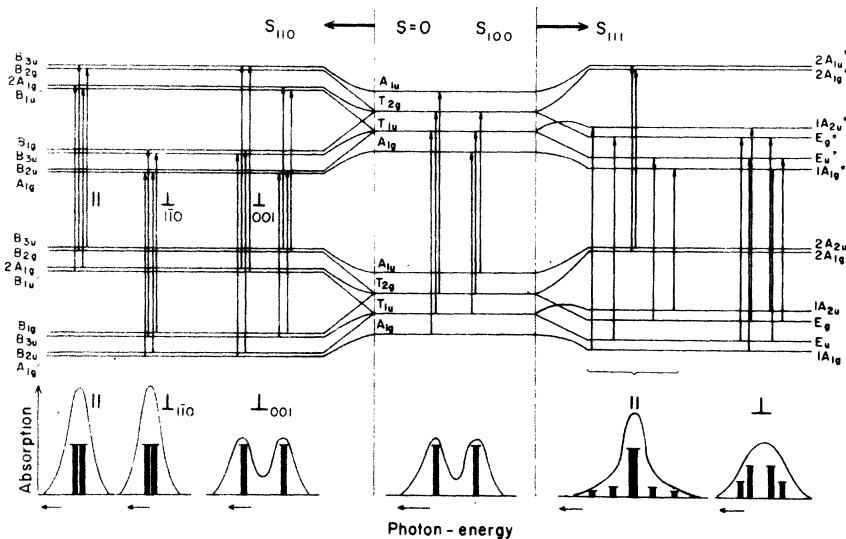
Vibrational Transitions of $\langle 111 \rangle$ Dipoles with Nearest-Neighbor Tunneling under Stress $S_{100}, S_{110}, S_{111}$ 

FIG. 11. Energy-level diagram and main optical transitions (with strength of order 1) for a $\langle 111 \rangle$ dipoles with nearest-neighbor tunneling under applied stress $S_{\langle 100 \rangle}$, $S_{\langle 110 \rangle}$, and $S_{\langle 111 \rangle}$. The resulting spectral transition histograms for \parallel and \perp polarization are indicated below.

original absorption band.¹⁰ In Table I we list the normalized second-moment changes $\langle \Delta U^2 \rangle_s / \langle \Delta U^2 \rangle_{S=0}$ of the main absorption, obtained (for $\alpha S \gg \Delta$) for $\langle 100 \rangle$, $\langle 111 \rangle$, and $\langle 110 \rangle$ elastic dipoles from the tunneling model. The predicted values of the second-moment changes lie between zero and the full, original second-moment contribution from tunneling (i.e., in the normalized values between 0 and -1). For the cases where the classical (zero-moment) stress alignment effect is vanishing due to symmetry (e.g., for $\langle 100 \rangle$ dipoles under $S_{\langle 111 \rangle}$), the quantum-mechanical elasto-optical effect is always zero, also. (This is different from the electric field case, treated in Paper I.) While for $\langle 100 \rangle$ and $\langle 111 \rangle$ dipoles only nearest-neighbor tunneling has been considered in Table I, for $\langle 110 \rangle$

dipoles we list both the case of nearest-neighbor (60°) and next-nearest-neighbor (90°) tunneling. As can be seen, the predicted values of the second-moment decreases are distinctly different for the two tunneling cases. Thus, from measurements of the anisotropy of the effect, the dipole orientation and predominant tunneling angle can be determined.

V. DISCUSSION AND INTERPRETATION OF EXPERIMENTAL RESULTS

A. Double structure of vibrational absorption

The first important new result is the appearance of a splitting of the CN^- vibrational absorption for diluted dipole systems at low temperature. We interpret this to be caused by the orientational

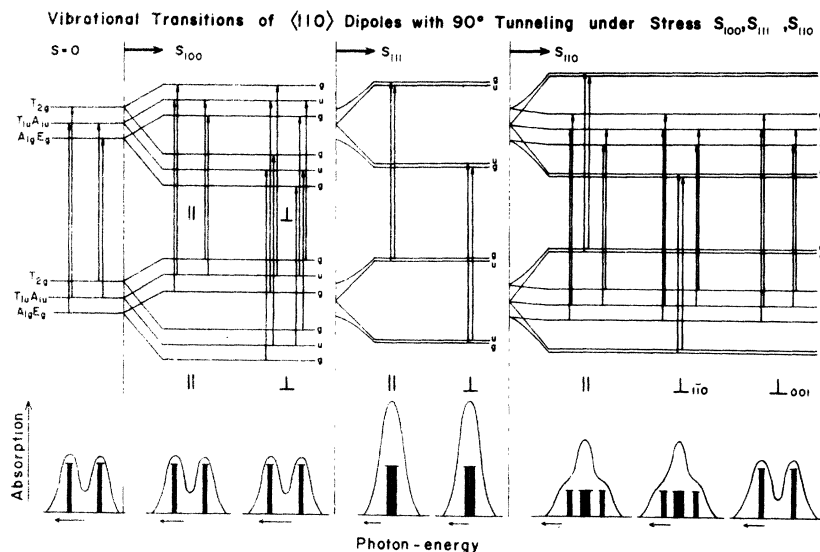


FIG. 12. Energy-level diagram and main optical transitions (with strength of order 1) for a $\langle 110 \rangle$ dipoles with next-nearest-neighbor (90°) tunneling under applied stress $S_{\langle 100 \rangle}$, $S_{\langle 111 \rangle}$, and $S_{\langle 110 \rangle}$. The resulting spectral transition histograms for the \parallel and the two inequivalent \perp polarizations are indicated below.

tunneling of the CN^- molecule, basing our arguments on the following points.

(i) The value for the tunneling splitting ($\Delta = 1-1.5 \text{ cm}^{-1}$), derived from other previous experiments,³ agrees very well with our observed optical splitting $\Delta E = 2.4 \text{ cm}^{-1} = 2\Delta$.

(ii) The most likely alternative explanation for the observed double structure would be the assumption of somehow perturbed CN^- surroundings with two slightly different potentials (force constants) for the CN^- vibration. For this case, the splitting should double in the second harmonic absorption, as compared to the fundamental. Within the accuracy of the experiments, however, the second harmonic absorption shows the same splitting as the fundamental absorption (Fig. 2).

(iii) The temperature variation in the relative strength of the Stokes and anti-Stokes component, expected for the proposed model, could be qualitatively observed (see, e.g., Fig. 1); resolution errors at the lowest temperatures, however, did not allow a quantitative check.

(iv) The drastic and highly anisotropic changes of the double structure under applied stress, discussed below, agree with the tunneling model and leave no other possibility for interpretation.

The CN^- molecule in KCl is the first solid-state system for which an orientational tunneling motion of a defect has been resolved in an optical experiment. This makes the KCl: CN^- system an important and unique test case for the tunneling model. The particular observed two-line structure allows some statements about the possible orientation of the CN^- dipoles in the octahedral crystal field. In Fig. 13 we compare the tunneling structure of $\langle 100 \rangle$, $\langle 111 \rangle$, and $\langle 110 \rangle$ dipoles (same structure in the ground and excited vibrational states), and the expected absorption histogram for the allowed transitions. For nearest-neighbor tunneling and a strong crystal potential, only $\langle 111 \rangle$ dipoles will produce a two-line spectrum, while $\langle 100 \rangle$ and $\langle 110 \rangle$ dipoles should display 4 and 5 components, respectively (Fig. 13). $\langle 110 \rangle$ dipoles with next-nearest-neighbor (90°) tunneling (which have been found for off-center Ag^+ ions),¹¹ however, are also expected to show a double structure. Thus, for strong crystal potentials, the double structure suggests nearest-neighbor tunneling $\langle 111 \rangle$ or next-nearest-neighbor tunneling $\langle 110 \rangle$ dipoles, while excluding nearest-neighbor tunneling $\langle 110 \rangle$ and $\langle 100 \rangle$ dipoles.

This situation changes if we leave the regime of a strong crystal potential, where the tunneling model is valid, and include the possibility of a very weak hindering potential. For $\langle 100 \rangle$ dipoles, e.g., the 2:1 ratio of the $\Delta_2:\Delta_1$ splitting (Fig. 13) will decrease with decreasing crystal-field param-

eter K . For $K = 16B$ (B is the rotational constant of CN^- molecule), derived in the earlier work,³ the splitting ratio $\Delta_2:\Delta_1$ would be 1.4, so that under only partial resolution the spectrum could show a two-component structure. Thus the observed double structure *alone* is not too decisive, excluding in a clear way only the $\langle 110 \rangle$ dipole 60° tunneling model.

B. Change of spectral shape under stress

The second important new result is the appearance of drastic and highly anisotropic spectral changes (narrowing effects) of the vibrational absorption under applied stress of various symmetry. For analysis, we compare the main effects, observed in \perp polarization [strong narrowing for $S_{\langle 110 \rangle}(\perp_{\langle 11\bar{1}0 \rangle})$, weaker narrowing for $S_{\langle 111 \rangle}$, and essential absence of narrowing for $S_{\langle 100 \rangle}$] to the second moment decreases, predicted by the tunneling model for different dipole orientations and tunneling angles (Figs. 10-12 and Table I). In doing so, the $\langle 100 \rangle$ dipole model fails completely: It predicts partial narrowing for $S_{\langle 100 \rangle}$ and absence of narrowing for $S_{\langle 111 \rangle}$ (both contrary to the experiment), and gives predictions for the two inequivalent polarizations \perp to $S_{\langle 100 \rangle}$, which are exactly opposite to the experimental behavior. Thus a $\langle 100 \rangle$ dipole model can be ruled out with a high degree of certainty. Similarly, a $\langle 110 \rangle$ dipole model with nearest-neighbor (60°) tunneling (already unlikely due to its expected five-component spectrum) fails in comparison to the observed material. A deci-

TABLE I. Normalized stress-induced second-moment changes $\langle \Delta U^2 \rangle_S / \langle U^2 \rangle_{S=0}$, derived from the tunneling model (for $kT \gg \alpha S \gg \Delta$).

Dipole	Stress	$\frac{\langle \Delta U^2 \rangle_S}{\langle U^2 \rangle_0} \parallel \text{polar.}$	$\frac{\langle \Delta U^2 \rangle_S}{\langle U^2 \rangle_0} \perp$
$\langle 100 \rangle$	$S_{\langle 100 \rangle}$	-1	-0.5
	$S_{\langle 111 \rangle}$	0	0
	$S_{\langle 110 \rangle}$	-0.5	-0.5 ($\perp_{\langle 110 \rangle}$) -1 ($\perp_{\langle 001 \rangle}$)
$\langle 111 \rangle$	$S_{\langle 100 \rangle}$	0	0
	$S_{\langle 111 \rangle}$	0	-0.5 -1 ($\perp_{\langle 110 \rangle}$)
	$S_{\langle 110 \rangle}$	-1	0 ($\perp_{\langle 001 \rangle}$)
$\langle 110 \rangle$ 60° tunnel.	$S_{\langle 100 \rangle}$	0	-0.5
	$S_{\langle 111 \rangle}$	-1	-0.25
	$S_{\langle 110 \rangle}$	-0.5	-0.5 ($\perp_{\langle 110 \rangle}$) 0 ($\perp_{\langle 001 \rangle}$)
$\langle 110 \rangle$ 90° tunnel.	$S_{\langle 100 \rangle}$	0	0
	$S_{\langle 111 \rangle}$	-1	-1
	$S_{\langle 110 \rangle}$	-0.5	-0.5 ($\perp_{\langle 110 \rangle}$) 0 ($\perp_{\langle 001 \rangle}$)

sion between the remaining two considered possibilities [$\langle 111 \rangle$ and $\langle 110 \rangle$ dipoles with nearest and next-nearest-neighbor tunneling, respectively] is more difficult, as both give qualitatively the same predictions for the existence or nonexistence of narrowing effects in \perp polarization: Both predict their presence for $S_{\langle 111 \rangle}$ and $S_{\langle 110 \rangle}(\perp_{\langle 1\bar{1}0 \rangle})$, and their absence for $S_{\langle 100 \rangle}$ and $S_{\langle 110 \rangle}(\perp_{\langle 001 \rangle})$. Qualitatively, however, their predictions are different: For $\langle 111 \rangle$ dipoles the $S_{\langle 110 \rangle}(\perp_{\langle 1\bar{1}0 \rangle})$ narrowing should be stronger than the $S_{\langle 111 \rangle}$ narrowing effects, while for $\langle 110 \rangle$ dipoles this order should be just reversed. The experiments, both in the fundamental and second harmonic absorption (Figs. 4-6), clearly show the first-mentioned order, thus deciding for the $\langle 111 \rangle$ dipole model.

C. Zero-moment absorption changes and elastic dipole moment

Besides the quantum-mechanical spectral effects due to the stress mixing of the tunneling states, discussed in Sec. VB, one expects the classical zero-moment absorption changes due to the stress alignment of the elastic dipoles. For $kT > \Delta$, these zero-moment changes from dipole alignment should be independent of the quantum effects and the same as for classical elastic dipoles [similar-

ly, as the electric susceptibility for tunneling dipoles is the same as that of classical dipoles ($\chi = Np^2/3kT$) for $kT > \Delta$].¹²

The measured integrated absorptions under stress of different symmetry (Fig. 9) reveal the following: (a) For light polarization \parallel to the applied stress the absorption strength decreases in all cases (if a change is observed). This clearly indicates that the CN^- defect is a "cigar-shaped elastic dipole." (b) Within the experimental accuracy, no change in absorption strength is observed for $S_{\langle 100 \rangle}$ in both \parallel and \perp polarization. This rules out a $\langle 100 \rangle$ dipole model and a $\langle 110 \rangle$ dipole model with any sizeable E_x elastic dipole component. (c) The absence of any absorption change for $S_{\langle 100 \rangle}(\perp_{\langle 001 \rangle})$ could be tested with high accuracy to large stress values (Fig. 9). This result is compatible only with a $\langle 111 \rangle$ dipole model. (d) For $S_{\langle 111 \rangle}$ and $S_{\langle 110 \rangle}$ in \parallel polarization, the absorption decrease approaches 66 and 100% of the initial absorption value, respectively, as expected for a $\langle 111 \rangle$ elastic dipole.¹³

Thus the anisotropy, sign and saturation values of the observed stress alignment dichroism are in agreement with a $\langle 111 \rangle$ dipole model, clearly excluding both the $\langle 100 \rangle$ and $\langle 110 \rangle$ alternative. In order to obtain an estimate of the elastic dipole

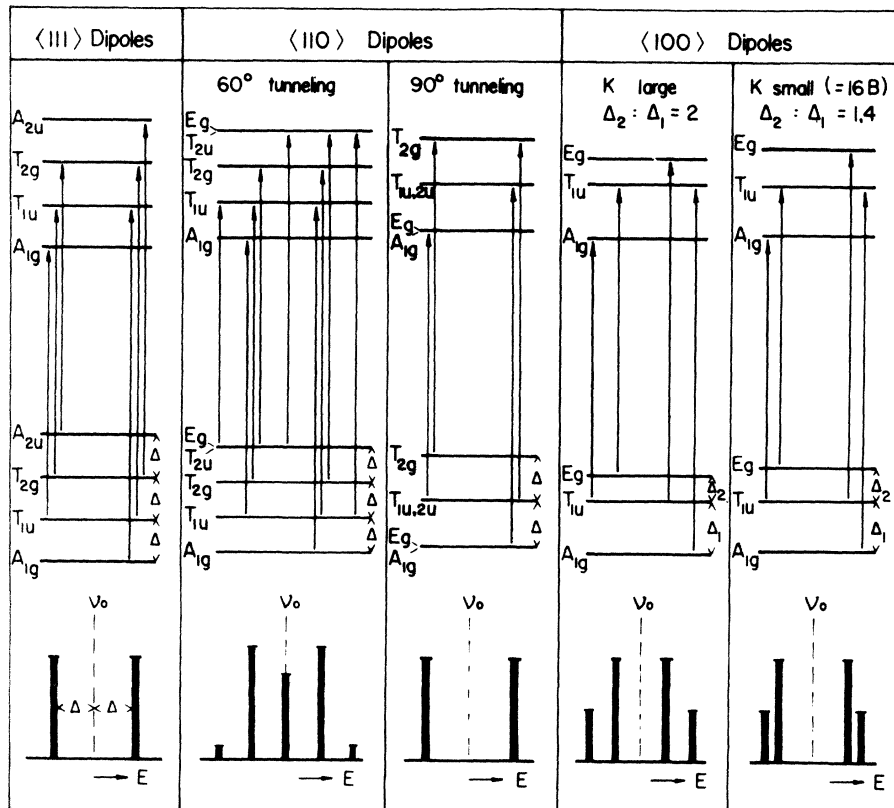


FIG. 13. Tunneling splitting of the vibrational ground and excited state for $\langle 111 \rangle$, $\langle 100 \rangle$, and $\langle 110 \rangle$ dipoles (the latter with nearest- and next-nearest-neighbor tunneling), and allowed optical transitions. For $\langle 100 \rangle$ dipoles, two situations with a strong crystal field parameter K ($\Delta_2 : \Delta_1 = 2$) and a weak crystal field ($\Delta_2 : \Delta_1 = 1.4$) are considered. The resulting spectral transition histograms are given in the lower part.

moment value, the measured curves for $S_{\langle 111 \rangle}$ (\parallel and \perp) and $S_{\langle 110 \rangle}$ (\parallel) in Fig. 9 were fitted to the calculated behavior of a cigar-shaped $\langle 111 \rangle$ oriented elastic dipole (full lines). The obtained parameters α , determining the stress splitting of the energy levels ($\Delta E = \alpha \times S$) are

$$\alpha_1 = 6.5 \times 10^{-24} \text{ cm}^3 \text{ (for } S_{\langle 111 \rangle}),$$

$$\alpha_2 = 7.7 \times 10^{-24} \text{ cm}^3 \text{ (for } S_{\langle 110 \rangle}).$$

For a $\langle 111 \rangle$ oriented rotationally symmetric defect with the elastic dipole components λ_1 and λ_2 , we expect

$$\Delta E_{\langle 111 \rangle} = \alpha_1 S_{\langle 111 \rangle} = \frac{8}{9} v_0 (\lambda_1 - \lambda_2) S_{\langle 111 \rangle},$$

$$\Delta E_{\langle 110 \rangle} = \alpha_2 S_{\langle 110 \rangle} = \frac{2}{3} v_0 (\lambda_1 - \lambda_2) S_{\langle 110 \rangle}.$$

With the measured values α_1 and α_2 and the volume of the primitive cell $v_0 = \frac{1}{4} a^3$, we obtain from

$$\alpha_1 (S_{\langle 111 \rangle}) (\lambda_1 - \lambda_2) = 0.126,$$

$$\alpha_2 (S_{\langle 110 \rangle}) (\lambda_1 - \lambda_2) = 0.183.$$

The difference in the value of the shape factor $\lambda_1 - \lambda_2$ is not quite unexpected: (a) Similar differences have been observed for $S_{\langle 111 \rangle}$ and $S_{\langle 110 \rangle}$ experiments even in cases with very accurate techniques (e.g., the EPR investigation of O_2^-).¹⁴ (b) Resolution errors can still be involved: For $S_{\langle 110 \rangle}$ (\parallel) the absorption band narrows strongly (see Table I), which under improper resolution conditions produces an apparent additional absorption decrease. This effect could give rise to a slope of the $S_{\langle 110 \rangle}$ curve, which is larger than the one expected for the reorientation dichroism.

In view of these uncertainties, we take as the result the mean value of the two measurements $(\lambda_1 - \lambda_2) = 0.15$, with an estimated accuracy of not better than $\pm 30\%$. The qualitative observation in Fig. 8 that the small sideband at 2100 cm^{-1} shows a stress alignment dichroism opposite to that of the main vibrational absorption, confirms its assignment to a vibration-libration combination band, for which one expects a π -polarized absorption and therefore a dichroism opposite to that of the σ -polarized vibrational band.

In summary we can state that the anisotropy of both the *second-moment changes* due to quantum-mechanical mixing of the tunneling states, and the *zero-moment changes* due to classical elastic dipole alignment give independent and decisive evidence for a $\langle 111 \rangle$ elastic dipole moment with the axis parallel to the CN^- molecule axis.

VI. COMPARISON WITH PREVIOUS WORK AND CONSEQUENCES

Our results agree with the high-temperature optical and the specific-heat data of Seward and

Narayanamurti (SN) in terms of the general conclusion, that CN^- molecules in KCl reorient in a weak crystalline potential and occupy at low temperatures, orientational ground states, characterized by a large ($\sim 1\text{-cm}^{-1}$) tunneling splitting. We disagree, however, with the low-temperature optical and elasto-optical data of SN and their interpretation in terms of the symmetry and shape of the CN^- elastic-dipole tensor.

(i) Instead of a single broad band (SN), we find at low temperatures a two-component spectrum, which is well separated for low CN^- concentrations. As the CN^- concentration, used by SN for the optical measurement (SN Fig. 3), was the same as our medium concentration in Fig. 2, improper resolution (rather than concentration effects) must have been the reason for the different results. The conclusion in SN and this work, derived from the unresolved or resolved broad absorption, is however the same: *a tunneling splitting of $\sim 1.2 \text{ cm}^{-1}$ for CN^- in KCl.*

(ii) Our elasto-optical data disagree with that of SN in two ways: (a) We find—in agreement with the tunneling model—pronounced *anisotropic second-moment changes* under stress application, which were not detected by SN. It should be noted that these changes of the band shape are very pronounced and well observable even for high CN^- concentrations, for which the double structure from tunneling is completely washed out. (See, for instance, the second harmonic absorption of very high CN^- concentrations under stress in Fig. 6.) (b) *The direction and anisotropy of our observed zero-moment changes* are opposite to that reported by SN: We find absorption *increases* for light polarization perpendicular to S (instead of decreases); while SN report large effects for $S_{\langle 100 \rangle}$ compared to $S_{\langle 111 \rangle}$, we find zero effect for $S_{\langle 100 \rangle}$ and a maximum change for $S_{\langle 111 \rangle}$. It should be noted that resolution errors cannot account for these differences: As for $kT > \Delta$ the zero-moment changes from classical elastic dipole alignment are independent of the (second moment) quantum effects, it is not necessary at all (in fact for experimental reasons not even desirable!) to resolve the tunneling structure and its detailed changes under stress, when measuring the stress-induced change of the integral absorption. For this reason our zero-moment measurements have been made with a medium CN^- concentration (the same as used by SN) and with a broadened slit-width (improved signal-to-noise ratio!) under intentionally reduced resolution conditions (see Figs. 7 and 8). It was tested, however that a variation of neither the CN^- concentration nor of the resolution changed the sign or anisotropy of the observed zero-moment effects.

In view of unexplained discrepancies under (ii a) and (ii b) between SN and our results, extreme care was taken to reproduce and double check all results under strict control (and, if possible, systematic variation) of all crystal and apparatus parameters. The essential consistency of our data in the fundamental and second harmonic absorption, obtained in two different spectrometers under very different conditions of resolution, optical density, crystal dimensions, dipole concentration and applied forces, should be mentioned as a strong support for the validity of our data. Changes in the general purity of the used crystal material (from reagent to ultrapure material) did not affect any of our results. Considerable efforts were made to compare the Utah and Cornell crystals, to check for any possible differences which could have caused the incompatible behavior. In all relevant features (like relative amount of unwanted CNO^- and OH^- admixture) the crystals were found very much comparable. In order to achieve a direct comparison, samples from the same crystal boule, used in the Cornell work, were kindly supplied to us by Pohl. They displayed—for the low CN^- concentration—exactly the same double structure and under stress application the same second- and zero-moment changes observed in our crystals.

Besides these experimental arguments, support for the validity of our results can be derived from their consistency with accepted physical models and valid considerations.

(a) The observed 2.4-cm^{-1} splitting of the absorption is expected for the tunneling splitting of $\Delta = 1.2\text{ cm}^{-1}$ derived from previous CN^- work. Not any of the known perturbation or interaction energies could account for a complete washing-out of this large splitting in a crystal with low dipole concentration.¹⁵

(b) Anisotropic second-moment decreases for an absorption with a width, determined by Δ , are a necessary consequence of the tunneling model, while their absence would contradict this model.

(c) A “cigar-shaped” elastic dipole, which we obtain, is expected for the CN^- defect from the elongated ellipsoidal shape of the CN^- molecule (derived from x-ray¹⁶ and neutron¹⁷ diffraction data in KCN and NaCN), and from the analogy to all known diatomic molecular elastic dipoles (like OH^- and O_2^-). The “pancake” shape of the elastic dipole, derived in SN, cannot be explained in any simple way.

An additional support for the correctness of our $\langle 111 \rangle$ dipole model for CN^- in KCl can be derived from the results of Kerr-effect measurements in $\text{KCl}:\text{CN}^-$ which will be published separately.¹⁸ The Kerr effect in the uv and visible range which

is Kramers-Kronig related to the electrochromism is found to be at least three orders of magnitude stronger for $\langle 111 \rangle$ fields compared to $\langle 100 \rangle$ electric fields. This very pronounced anisotropy of the electrooptical effect proves unquestionably that the CN^- electric dipole has a $\langle 111 \rangle$ orientation, in KCl, in agreement with our elasto-optical result.

Every work on the $\text{KCl}:\text{CN}^-$ system since 1966 has quoted the elasto-optical results from SN as the evidence for a $\langle 100 \rangle$ defect model, and has accordingly based its discussion and interpretation on a $\langle 100 \rangle$ orientation of the CN^- electric dipole axis. A change to a $\langle 111 \rangle$ model, which we postulate here, therefore affects the interpretation of a large number of investigations on this system from the last 8 years. Thus we have to ask, if our proposed $\langle 111 \rangle$ model is in principle consistent with the results of these investigations, or leads to any decisive contradictions:

(i) The integrated specific-heat anomaly ΔS of CN^- defects in KCl was found close to $\Delta S = Nk \ln 6$, which was taken as a confirmation of the sixfold $\langle 100 \rangle$ dipole model.³ A $\langle 111 \rangle$ dipole model with $\Delta S = Nk \ln 8$ would produce, however, only a 15% higher ΔS effect, and it can be reasonably assumed that the combined errors from the chemical analysis for N and from the specific heat measurement and extrapolated integration, can easily be 15% or larger. [In this connection it should be noted that for the off-center Li^+ defect with its very securely determined $\langle 111 \rangle$ symmetry the integration of the (perfectly Schottky shaped) ΔS anomaly gave similarly a value,¹⁹ which is by ~25% too low compared to the expected $Nk \ln 8$ value.]

(ii) Field and Sherman²⁰ calculated the interaction potential for the CN^- defect and obtained $\langle 111 \rangle$ potential minima with barrier heights of 90 cm^{-1} . They discard this “apparently anomalous result” in view of the $\langle 100 \rangle$ dipole model, derived by SN, explaining the failure of their calculation by the possible presence of strong anisotropic lattice distortions around the CN^- defect, which may change the potential minima from $\langle 111 \rangle$ to $\langle 100 \rangle$. With the new $\langle 111 \rangle$ dipole model, their original calculation (including the barrier height) may look more reasonable.

(iii) The electric field effect on the CN^- vibrational absorption was reported by Pompi and Narayanamurti^{4,5} to consist of zero-moment absorption changes, with a direction opposite to the one expected for a diatomic dipole vibrator. The interpretation of these data was given by a $\langle 100 \rangle$ dipole model within a “modified Devonshire scheme.” As the electric dipole moment p of the CN^- is very small and all measurements were

done in the range $pE < \Delta$, these results disagree with the tunneling model which predicts in this range strong changes of the absorption *shape* rather than the absorption *integral*. A reinvestigation of this problem, currently under way in this laboratory, yields indeed results²¹ which are in complete disagreement with the previously reported field dichroism data, but are in agreement with the predictions from the $\langle 111 \rangle$ dipole tunneling model.

(iv) *Ultrasonic velocity and attenuation* experiments on CN^- defects were performed by Byer and Sack^{6,7} and extended by Welsh.²² The main result of this very careful and methodical investigation is a strong coupling of the CN^- defects to T_{2g} stress, compared to a very weak coupling to E_g stress. In spite of this clear finding, which indicated basically a $\langle 111 \rangle$ elastic dipole, these results were not used to discard the $\langle 100 \rangle$ model, derived from the ir work. Instead, complicated and questionable models, with perpendicular electric and elastic dipole axes, have been constructed and discussed, in order to integrate the contradictory ir and acoustic results into a single model. Our new $\langle 111 \rangle$ model allows a natural and straightforward interpretation of the Byer and Sack data, yielding quantitative agreement to our elasto-optical results: The strong coupling to T_{2g} stress is produced by a $\langle 111 \rangle$ oriented rotationally symmetric elastic dipole tensor; Byer and Sack determined from the measured T_{2g} compliance change a shape factor $|\lambda_1 - \lambda_2| = 0.156$, which is in very good agreement with the mean value $\lambda_1 - \lambda_2 = 0.15$ obtained from our elasto-optical measurements.

The small E_g part of the elastic dipole, measured by Byer and Sack, may be due to the fact that the strict selection rules for classical elastic dipoles, as derived by Nowick and Heller,²³ become somewhat modified for quantum-mechanical dipoles in weak crystal potentials. This problem was theoretically investigated by Welsh²² who showed for instance that a $\langle 111 \rangle$ dipole in a weak crystal potential will have a small E_g elastic dipole part admixed to its essential T_{2g} part. The accuracy of our elasto-optical experiment (Fig. 9) is not sufficient to decide if a small zero-moment effect is present for $S_{\langle 100 \rangle}$.

The confirmation of the acoustically determined elastic dipole value for CN^- in KCl and its clear attribution to a $\langle 111 \rangle$ model by optical techniques, make it almost certain that the other CN^- systems for which a stress coupling $T_{2g} \gg E_g$ has been found in the acoustic work (CN^- in KBr and KI) will be $\langle 111 \rangle$ oriented defects too.

(v) The *dielectric measurements* on $\text{KCl}:\text{CN}^-$ by Sack and co-workers^{24,25} showed a Curie-law

behavior for ϵ_1 , yielding an electric dipole moment of $p = 0.3$ Debye. Due to the small value of this moment, the polarization is isotropic and independent of the dipole symmetry, so that the dielectric experiments are neither conclusive about nor dependent on a possible $\langle 100 \rangle$ or $\langle 111 \rangle$ dipole model.

(vi) *Raman studies* on CN^- in KCl by Callender and Pershan²⁶ gave clear evidence of scattering from rotational degrees of freedom of the CN^- molecule. The details of the observed Raman spectra have been interpreted, following the SN model, in terms of $\langle 100 \rangle$ dipoles in a $K > 0$ Devonshire scheme with reasonable success. Not any alternative model was tried for interpretation, so that it is not clear how well a $\langle 111 \rangle$ model could account for the data as well.

(vii) An investigation of the CN^- tunneling states using the *spin-phonon interaction* by Hetzler and Walton²⁷ yielded two resonances at $E_1 = 1.1 \text{ cm}^{-1}$ and $E_2 = 2.0 \text{ cm}^{-1}$ in agreement with a tunneling model for a $\langle 100 \rangle$ dipole. Our $\langle 111 \rangle$ model would predict a third resonance transition at about $E_3 = 3E_1$. Hetzler and Walton observe indeed a third resonance at 3.2 cm^{-1} , which they however discard as an "experimental artifact," because it was found to be sample dependent.

VII. CONCLUSIONS

The work presented here should be regarded only as a "first-order approximation" to the problem, which suffers still from many shortcomings. As it had to be done under severe optical resolution and signal-to-noise limitations with a commercial ir instrument, it did not allow the resolution of all the transitions under stress predicted by the tunneling model (Figs. 10–12). Therefore, many details of the predicted behavior (like the tuning of paraelectric sidebands out of the absorption center by stress) could not be explicitly tested. The treatment given here may still be a valuable model case for situations in which a smaller tunneling splitting (or limited resolution conditions) does not allow the resolution of the fine structure, but does allow to observe the spectral changes. Similar to the case of phonon-broadened optical transitions without resolved phonon structure, the treatment of the *moment changes* of the bands is apparently a very effective way to describe the effects of applied perturbations. Our treatment of this aspect has been very empirical and is still incomplete; clearly a more refined and comprehensive, theoretical treatment of this problem (similar to the elegant method-of-moment treatment of phonon-broadened optical transitions by Henry,

Schnatterly and Slichter²⁸) would be very desirable.

For the KCl:CN⁻ with its large tunneling splitting all transitions under field and stress should be resolvable, so that the moment approach given here could be replaced by a full analysis of the individual transition components. Measurements, which are directed towards this goal, are presently under way in this laboratory by Beyeler, using optical high-resolution techniques and cooled InSb detectors. The preliminary results of this work confirm with high accuracy the 2.4-cm⁻¹ splitting of the CN⁻ absorption in KCl reported here, and show a similar, but smaller, splitting in other host materials.²¹ It moreover shows that resolution of all the optical transitions under applied stress is indeed possible,²⁹ confirming the $\langle 111 \rangle$ cigar-shaped elastic dipole model, proposed here. The full account of this work, which is well in progress, will therefore test and further develop the $\langle 111 \rangle$ dipole tunneling model by a fully resolved "paraelastic-resonance spectroscopy of the vibrational absorption" with an unprecedented accuracy.

ACKNOWLEDGMENTS

Clarifying discussions on the earlier CN⁻ work with Professor R. O. Pohl and Professor W. D. Seward, and Dr. Narayanamurti, as well as discussions with Dr. H. U. Beyeler on the present work are gratefully acknowledged.

APPENDIX: STRESS EFFECTS ON THE TUNNELING MATRIX ELEMENT

We have conducted all our discussions in the framework of the usual tight-binding tunneling approximation, which assumes that the tunneling matrix element for the reorientation of the defect is *not* changed by the applied perturbation (E or S). While this is possibly valid for the OH⁻ in electric field (treated in Paper I), this approximation should break down for the weakly hindered CN⁻ rotator. With the obtained elastic dipole value and stresses up to 700 atm, we reach stress splitting energies up to 35 cm⁻¹ (for $S_{\langle 110 \rangle}$, which definitely is no longer a small quantity compared to the expected barrier height of 50–100 cm⁻¹). Thus one can expect a stress dependent tunneling matrix

element $\Delta(S)$, which means for our spectral investigation the expectation of *stress-induced second-moment changes of the total absorption*. This effect will superimpose on the second moment changes of the main vibrational absorption due to the stress mixing of the tunneling states, on which we have focused our attention in this work. These latter effects, which we have considered, are characterized by the fact that they are always second moment *decreases*, and that they occur for relatively small stress, when αS is comparable in magnitude to Δ . The $\Delta(S)$ effects, on the other hand, will most clearly be detectable for very large stress, and are expected to consist of either second moment increases or decreases (because the stress can both increase or decrease the tunneling probability).

Examples for this $\Delta(S)$ effect can be seen in several of the presented curves: (a) While for the tunneling model with constant Δ no effects are expected for $\langle 111 \rangle$ dipoles under $S_{\langle 100 \rangle}$, we observe a small narrowing effect (which continues to large S values) for \perp polarization (Fig. 3) and a sizeable broadening effect (not shown here) for \parallel polarization. (b) Similarly we observe for $S_{\langle 111 \rangle}$ (aside of the initial stress-mixing narrowing effect in the $\alpha S \approx \Delta$ range) a further narrowing for large stress (indicated in Fig. 7 by the fact that the absorption seems to come into scale again due to serious resolution errors by the narrowing band). For \parallel polarization a considerable broadening effect is observed. (c) For $S_{\langle 110 \rangle}$ and $\perp_{\langle 001 \rangle}$ polarization (expected to be invariant in the $\Delta = \text{constant}$ model) a broadening effect is observed (Fig. 8). Measurement with high resolution show that in the observed cases of broadening [$S_{\langle 100 \rangle}(\parallel)$, $S_{\langle 111 \rangle}(\parallel)$, and $S_{\langle 110 \rangle}(\perp_{\langle 001 \rangle})$] the two components of the initial double structure are preserved and separate further under applied stress [Fig. 5(b) gives an example]. For the case of $S_{\langle 100 \rangle}(\parallel)$ the separation could be tuned by the stress by a factor of 3 (from 2.4 to 7.5 cm⁻¹)! Thus, the optical technique allows to probe in detail how stress of different symmetry changes the tunneling motion along different directions in the crystal (selected by the light polarization.) Detailed studies on these effects are under way and will be published separately.

*Work supported by NSF Grant No. GH33704X. Helium gas was provided by a departmental grant from ONR.

¹F. Lüty, preceding paper, Phys. Rev. B **10**, 3667 (1974).

²For a review of previous CN⁻ work and its interpretation, see V. Narayanamurti and R. O. Pohl, Rev. Mod. Phys. **42**, 201 (1970).

³W. D. Seward and V. Narayanamurti, Phys. Rev. **148**, 463 (1966).

⁴R. L. Pompi and V. Narayanamurti, Solid State Commun. **6**, 645 (1968).

⁵R. L. Pompi, Ph.D. thesis (Cornell University, 1968) (unpublished).

- ⁶N. E. Byer and H. S. Sack, *Phys. Status Solidi* **30**, 569 (1968).
- ⁷N. E. Byer and H. S. Sack, *Phys. Status Solidi* **30**, 579 (1968).
- ⁸H. Härtel, *Phys. Status Solidi* **42**, 369 (1970).
- ⁹S. Brodersen, *J. Opt. Soc. Am.* **44**, 22 (1954).
- ¹⁰We neglect possible shifts of the vibrational transition energy $h\nu_0$, caused by stress-induced changes of the lattice parameter. They will add changes of the first absorption moment, which, however, are unimportant for our considerations about quantum-mechanical effects.
- ¹¹S. Kapphan and F. Lüty, *Phys. Rev. B* **6**, 1537 (1972).
- ¹²H. Shore, *Phys. Rev.* **151**, 570 (1966).
- ¹³The only systematic deviation of any appreciable size between measured and calculated behavior occurs for large S value of the $S_{\langle 110 \rangle}$ (\parallel) case, where the absorption should disappear completely. The very small observed residual absorption ($\approx 10\%$) can possibly be accounted for by the not quite perfect polarization-characteristic of the used wire-grid polarizer. Two wire-grid polarizers showed at 2090 cm^{-1} an intensity ratio for crossed and parallel position $I_{\perp}/I_{\parallel} \approx 0.15$. Thus it is likely that the small residual absorption was caused by a small admixture of \perp polarized light to the \parallel polarized light.
- ¹⁴W. Känzig, *J. Phys. Chem. Solids* **23**, 479 (1962).
- ¹⁵One can show, for instance, that a particular background stress of the usually assumed magnitude ($S_{\langle 111 \rangle} \leq 30\text{ atm}$, producing a level splitting of $\Delta E \leq 1\text{ cm}^{-1}$) averaged over \parallel and \perp optical transitions, will still keep the double structure of the absorption essentially preserved, though making it somewhat smeared out.
- Background electric fields of the usually assumed magnitude (several 10^4 V/cm) should not affect the absorption shape at all, due to the very small CN^- electric dipole moment.
- ¹⁶J. M. Bijvoet and J. A. Lely, *Rec. Trav. Chem.* **59**, 908 (1940).
- ¹⁷N. Elliot and J. Hastings, *Acta Crystallogr.* **14**, 1018 (1961).
- ¹⁸A. Diaz-Gongora and F. Luty, *Solid State Commun.* (to be published).
- ¹⁹J. P. Harrison, P. P. Peressini, and R. O. Pohl, *Phys. Rev.* **171**, 1037 (1968).
- ²⁰G. R. Field and W. F. Sherman, *J. Chem. Phys.* **47**, 2378 (1967).
- ²¹H. U. Beyeler, *Bull. Am. Phys. Soc.* **19**, 105 (1974), and unpublished.
- ²²F. S. Welsh, Ph.D. thesis (Cornell University, 1969) (unpublished).
- ²³A. S. Nowick and W. R. Heller, *Adv. Phys.* **14**, 101 (1965).
- ²⁴H. S. Sack and M. C. Moriarty, *Solid State Commun.* **3**, 93 (1965).
- ²⁵A. Lakatos and H. S. Sack, *Solid State Commun.* **4**, 315 (1965).
- ²⁶R. Callender and P. S. Pershan, *Phys. Rev. A* **2**, 672 (1970).
- ²⁷M. C. Hetzler and D. Walton, *Phys. Rev. B* **8**, 4801 (1973).
- ²⁸C. H. Henry, S. E. Schnatterly, and C. P. Slichter, *Phys. Rev.* **137**, A583 (1965).
- ²⁹H. U. Beyeler, *Bull. Am. Phys. Soc.* **19**, 328 (1974), and unpublished.